Published in final edited form as:

Health Phys. 2020 November ; 119(5): 647–658. doi:10.1097/HP.0000000000001352.

IMMUNE RECONSTITUTION AND THYMIC INVOLUTION IN THE ACUTE AND DELAYED HEMATOPOIETIC RADIATION SYNDROMES

Tong Wu[1], **P. Artur Plett**[1], **Hui Lin Chua**[1], **Max Jacobsen**[2], **George E. Sandusky**[2], **Thomas J. MacVittie**[3], **Christie M. Orschell**[1]

[1]Department of Medicine, Indiana University School of Medicine, Indianapolis, IN

[2]Department of Pathology and Laboratory Medicine, Indiana University School of Medicine, Indianapolis, IN

[3]Department of Radiation Oncology, University of Maryland School of Medicine, Baltimore, MD

Abstract

Lymphoid lineage recovery and involution after exposure to potentially lethal doses of ionizing radiation have not been well defined, especially the long-term effects in aged survivors and with regard to male / female differences. To examine these questions, male and female C57BL/6 mice were exposed to lethal radiation at 12 weeks of age in a model of the Hematopoietic-Acute Radiation Syndrome, and bone marrow, thymus, spleen and peripheral blood examined up to 24 months of age for the lymphopoietic Delayed Effects of Acute Radiation Exposure. Aged mice showed myeloid skewing and incomplete lymphocyte recovery in all lymphoid tissues. Spleen and peripheral blood both exhibited a mono-phasic recovery pattern while thymus demonstrated a bi-phasic pattern. Naïve T cells in blood and spleen and all subsets of thymocytes were decreased in aged irradiated mice compared to age-matched non-irradiated controls. Of interest, irradiated males experienced significantly improved reconstitution of thymocyte subsets and peripheral blood elements compared to females. Bone marrow from aged irradiated survivors was significantly deficient in the primitive lymphoid-primed multipotent progenitors and common lymphoid progenitors, which were only 8–10% of levels in aged-matched non-irradiated controls. Taken together, these analyses define significant age- and sex-related deficiencies at all levels of lymphopoiesis throughout the lifespan of survivors of the Hematopoietic-Acute Radiation Syndrome, and may provide a murine model suitable for assessing the efficacy of potential medical countermeasures and therapeutic strategies to alleviate the severe immune suppression that occurs after radiation exposure.

Keywords

Health effects (radiation effects); mice; whole body irradiation; bone marrow

CORRESPONDING AUTHOR: Name: Christie M. Orschell, Address: 980 W. Walnut St., R3-C341, Indianapolis, IN, 46202, Phone: 317-278-2834, Fax: 317-274-0396, corschel@iu.edu.

CONFLICTS OF INTEREST AND SOURCES OF FUNDING:
The authors have no conflicts of interest to declare.

INTRODUCTION

The acute radiation syndromes (ARS) and the delayed effects of acute radiation exposure (DEARE) in survivors of ARS are serious and potentially lethal outcomes of exposure to high-dose radiation. Treatments for the hematopoietic-ARS (H-ARS) include the recently approved medical countermeasures (MCM) Neupogen (granulocyte colony stimulating factor, G-CSF), Neulasta (pegylated G-CSF), and Leukine (GM-CSF) (Singh and Seed 2020), which stimulate primitive hematopoietic progenitor cells to produce life-saving blood elements, primarily of the myeloid lineage (Plett et al. 2012, Farese et al. 2013, Chua et al. 2014, Hankey et al. 2015, Satyamitra et al. 2017). Although these MCM significantly increase survival from H-ARS, they do little to alleviate the morbidity of DEARE and its devastating multi-organ dysfunction, including long-term hematopoietic insufficiency.

One of the most serious consequences of hematopoietic DEARE is defective lymphocyte reconstitution and its subsequent immune insufficiency. Survivors of H-ARS often suffer from long-term T-cell deficiencies that dampen robust protective immune responses, including decreased T-cell number, imbalanced CD4/CD8 ratio, and compromised naive T-cell receptor diversity (Dainiak et al. 2003). Long term survivors, as well victims of the atomic bombings of Hiroshima and Nagasaki (Sasaki et al. 1991, Kamiya et al. 2015) and cancer patients that have received radiotherapy (Bhatia et al. 1996), also experience increased incidence of infections and cancer, likely due to deficient T-cell surveillance (van Heijst et al. 2013). Many of these immune perturbances also occur to a lesser degree during normal aging in association with thymic involution. Thymic involution, the age-related loss of thymic mass and reduction of naïve T cell output, correlates with reduced immune surveillance and onset of cancers, autoimmunity, and infectious diseases in aging (Rezzani et al. 2014). Age-related thymic involution and its associated immune dysfunction are exacerbated by previous radiation exposure, further compounding the immune deficiencies in hematopoietic DEARE.

While immune dysfunction has been well characterized in normal aging (Denkinger et al. 2015), as well as in the acute phase of radiation exposures, little is known regarding the immune suppression that occurs during DEARE. Generation of functional immunity is a complex process. Briefly, bone marrow (BM) long-term hematopoietic stem cells (LT-HSC) differentiate into multipotent progenitors (MPP), followed by lymphoid-primed multipotent progenitors (LMPP), and then common lymphoid progenitors (CLP). LMPP and CLP emigrate from the BM to the thymus where they differentiate into CD4-CD8- double negative (DN) cells, followed by CD4+CD8+ double positive (DP) cells, and finally single positive CD4+ or CD8+ T cells. Mature CD4+ and CD8+ T cells migrate from the thymus into peripheral blood (PB) and secondary lymphoid organs, where they initiate immunosurveillance. Due to the rapid proliferation and turnover of thymocytes, the thymus is highly radiosensitive. Remaining CLP in the BM develop into mature B cells (Germain 2002, Zlotoff and Bhandoola 2011).

The authors have previously developed a well-characterized murine model of H-ARS and DEARE in young adult C57BL/6 mice, and have used this model to study mechanisms and efficacy of MCM against radiation for licensure and treatment strategies (Plett et al. 2012,

Shakhov et al. 2012, Hoggatt et al. 2013, Chua et al. 2014, Garrett et al. 2014, Plett et al. 2014, Plett et al. 2015, Unthank et al. 2015, Fish et al. 2016, Dynlacht et al. 2017, Chua et al. 2019, Garrett et al. 2019, Jones et al. 2019, Unthank et al. 2019). Herein, the authors have characterized the prolonged immunosuppression at all levels of lymphocyte development in these acute and chronic radiation models. Data presented here aim to increase understanding of the severe immune dysfunction that occurs in radiation survivors, with the ultimate goal of generating a mouse model suitable for assessing the efficacy of potential MCM and therapeutic strategies.

MATERIALS AND METHODS

Mice

Specific pathogen-free C57BL/6 mice (50:50 male:female; Jackson Laboratory, Bar Harbor, Maine, United States) were received at 10 weeks of age and acclimated for 2 weeks prior to irradiation. All studies were approved by our Institutional Animal Care and Use Committee.

Study design

Irradiated (IR) mice analyzed in these studies were vehicle controls from 54 MCM screening studies performed over a period of 9 years (2010–2018), and are referred to herein as “IR”. Non-irradiated (NI) age- and sex-matched mice aged along with the IR mice served as controls. Husbandry and health status monitoring were carried out as previously described (Plett et al. 2015, Chua et al. 2019). Surviving mice at d30 post-IR were allowed to age in our animal facility for up to 24 mo. of age [21 mo. post-total body irradiation (TBI)]. Between days 1–30 (d1–30) post-irradiation (post-IR), mice were provided with autoclaved acidified water and wet feed ad libitum. Autoclaved acidified water was changed to non-acidified non-autoclaved reverse osmosis water after d30 and throughout the DEARE phase. Subgroups of aging mice were euthanized at defined time points and assessed for immune parameters as described herein. Some aging mice required humane euthanasia due to ulcerative dermatitis, labored breathing, severely hunched posture, inactivity, neurological symptoms or the presence of abnormal growths negatively affecting movement.

Irradiation and dosimetry

Irradiation and dosimetry were performed as previously described (Plett et al. 2015, Chua et al. 2019). Mice were exposed cranial-caudal on a rotating platform to single uniform TBI doses of 8.72 (estimated LD70/30) or 9.04 Gy (estimated LD90/30) (Plett et al. 2015) gamma radiation from a stationary ^{137}Cs radiation source (Mark 1 Irradiator, JL Shepherd, San Fernando, California, United States) at an exposure rate of 0.93–1.03 Gy min^{-1}. Since there were no differences in the experimental outcomes assessed in these studies between the LD70/30 and LD90/30, data from mice exposed to either dose were combined.

Complete blood cell counts (CBC)

Peripheral blood from tail snips was collected into an EDTA-coated capillary tube and analyzed for CBC using a validated HEMAVET® 950FS Hematology System (Drew Scientific, Waterbury, Connecticut, United States), as previously described (Plett et al.

2014). To minimize stress effects, mice were bled no less than 14 days apart during H-ARS (Plett et al. 2012, Plett et al. 2015).

Tissue harvest and single cell suspensions

All tissues were harvested following euthanasia by CO_2 or isoflurane inhalation, as previously described (Unthank et al. 2015, Unthank et al. 2019). Thymi were carefully cleared of fat and connective tissue under a dissecting microscope to eliminate contamination with non-thymic tissue. Thymus and spleen weights were obtained using a Mettler Toledo Balance XS204 (Mettler-Toledo LLC, Columbus, Ohio, United States). Single cell suspensions of thymocytes and splenocytes were generated by macerating tissues between the frosted ends of two microscope slides or with the blunt end of a syringe plunger, respectively. Peripheral blood was collected from tail snips and bone marrow cells were flushed from femurs, tibias, pelvis, and humeri. Erythrocytes were removed from samples by ammonium chloride lysis.

Tissue fixation, histological staining, and imaging

Thymi and spleens were fixed in neutral buffered formalin (NBF) overnight. Formalin-fixed tissues were paraffin embedded and sectioned, then stained with hematoxylin/eosin (H&E) and Picrosirius red. For H&E sections, digital images were acquired using an Aperio Scan Scope CS system (Aperio, Inc., Vista, California, United States). For Picrosirius red sections, digital images were acquired using a Leica DM 5000B microscope (Leica Microsystems, Inc., Buffalo Grove, Illinois, United States) with a Diagnostic Instruments Spot RTKE camera (SPOT Imaging Solutions, Sterling Heights, Michigan, United States) (Unthank et al. 2015, Vogel et al. 2015). For quantifying the Picrosirius red stained thymus tissue, 4–6 images were obtained randomly per slide at 5X magnification. All images were analyzed using ImageJ (version 1.50v; National Institutes of Health). Red, green, and blue (RGB) images were converted to grayscale then percentage of red-stained collagen in the background of pale-stained medullar area was measured. More measurement information can be found on the ImageJ NIH website.

Flow cytometric analyses

$B220^+$ B cells were identified using B220-PE-Texas Red or APC, $CD4^+$ T cells by CD4-APC or PECY5, and $CD8^+$ T cells by CD8a-PE or Pacific Blue. Naïve $CD4^+$ and $CD8^+$ T cells ($CD44^{lo}$ $CD62L^{hi}$) were detected using the additional antibodies CD44-APCCY7 and CD62L- PerCPCY5–5. Double negative thymocytes were defined as $CD4^-$ $CD8^-$ and subdivided into DN1, DN2, DN3, and DN4 based on expression of CD44 and CD25 as follows: DN1: $CD44^+$ $CD25^-$; DN2: $CD44^+$ $CD25^+$; DN3: $CD44^-CD25^+$; DN4: $CD44^-CD25^-$ using CD4-PerCPCY5–5, CD8-PE or Pacific Blue, CD44-APC or APCCY7 and CD25-PECY7 antibodies. Bone marrow LMPP cells [Lin^- ($Ter119^-$ $CD3^-$ $Gr1^-B220^-$ $CD11b^-$) c-Kit^{hi} Sca-1^{hi} $Flt3^{hi}$ $CD34^+$] and CLP (Lin^- c-Kit^{int} Sca-1^{int} $IL7R^+$ $Flt3^{hi}$) were identified using CD11b-FITC, Ter119-FITC, CD3-FITC, Gr1-FITC, B220-FITC, Sca-1-PECY7 or BV650, c-Kit-APC, CD34-Pacific Blue or BV421, IL7R-APCCY7 and FLT3-PE or PECY5 antibodies. Antibodies were purchased from BD Biosciences (San Jose, California, US; CD4-APC, CD4-PECY5, CD8a-PE, CD8-Pacific Blue, CD62L-PerCPCY5–5, CD4-PerCPCY5–5, CD44-APC, CD11b-FITC, Ter119-FITC, CD3-FITC, Gr1-FITC,

B220-FITC, CD34-BV421 and Sca-1-BV650), eBiosciences (San Diego, California, US; CD44-APCCY7, CD34-Pacific Blue, IL7R-APCCY7, FLT3-PE and FLT3-PECY5) or Biolegend (San Diego, California, US; CD25-PECY7, Sca-1-PECY7 and c-Kit-APC). The staining processes were carried out for 20 mins at 4°C in the dark, followed by washing with 1% bovine calf serum/PBS. Samplers were acquired using a BD LSRII system (Becton Dickinson, Franklin Lakes, New Jersey, United States) and analyzed using Flow Jo Software.

Statistical analysis

Unpaired Student's t-tests were performed to compare the following parameters: CBC, thymus and spleen weight and cellularity, thymic collagen deposition, and lymphoid cell types. If no sex difference was observed, data from males and females were combined. While many parameters measured over time were also significantly different at individual time points, a single asterisk denoting significance comparing all mice over a specific time range was used rather than multiple asterisks at individual time points, for the ease of the reader. Data are expressed as mean ± standard error of the mean (SEM). $P<0.05$ was considered significant.

RESULTS

Reconstitution and involution of peripheral blood cells

The authors have previously documented significantly decreased numbers of all blood elements in the PB of aged H-ARS survivors compared to NI age-matched controls (Chua et al. 2019). To investigate male / female differences in the decreased blood production in H-ARS survivors, as well as in normal aging in NI age-matched controls, PB CBC from males and females were examined separately. The fluctuation in animal number during the course of the study is due to the fact that these are retrospective analyses that combined data from several studies, and also because mortality increases with age, especially in radiation survivors, leaving fewer aged mice available for analyses at later time points. When CBC from NI male or NI female mice of multiple ages between 3 mo. and 24 mo. were compared, white blood cell (WBC), neutrophil (NE), lymphocyte (LY), and platelet (PLT) were all found to be significantly higher in NI males compared to females (Fig. 1a–e). In IR mice, all blood parameters were significantly reduced during the H-ARS phase, as we and others have reported (Patchen 1995, Plett et al. 2012, Plett et al. 2014), and did not differ between males and females. However, sex differences in CBC became again apparent as H-ARS survivors aged. When data from IR males or IR females between 6 and 21 months post-TBI were compared, all blood elements [WBC, NE, LY, red blood cell (RBC), and PLT] were found to be significantly decreased in IR females compared to IR males (Fig. 1a–e). Neutrophils gradually increased in the DEARE phase in both IR males and IR females (Fig. 1b), whereas LY declined over time, most dramatically in IR females (Fig. 1c). A similar trend was observed in NI mice during aging, in which NE increased and LY decreased (Fig. 1b & 1c), indicative of myeloid skew. The enhanced radiosensitivity of LY compared to other blood elements is evidenced by the sustained lymphopenia at the end of the H-ARS phase (d30 post-TBI) compared to the nearly complete recovery of most other blood elements (Fig. 1a–e).

Reconstitution and involution of thymus and spleen

Lymphocytes originate in the BM from the LT-HSC and migrate as LMPP and CLP to the thymus, where they continue maturation to become mature CD4+ and CD8+ T lymphocytes. Given the high degree of radiosensitivity of the thymus (Takada et al. 1969, Huiskamp et al. 1983), and potential impact of radiation-induced thymic damage on long-term T cell maturation, thymus weight and cellularity in IR mice were examined during the H-ARS and DEARE phases in comparison to NI age-matched controls.

Thymus weight and cellularity were found to be significantly greater in young 12 week old (w/o) NI female mice compared to young males (Figs. 2a and 2b), in agreement with others (Gui et al. 2011, Guo et al. 2017). However, as NI mice aged, thymus weight and cellularity gradually decreased in both sexes, and sex differences in geriatric mice lessened with age, similar to other reports (Sempowski et al. 2002, Guo et al. 2017).

During the H-ARS phase, thymic weight and cellularity changed in a biphasic pattern, with nadirs at d3 and d20 post-IR and a transient peak at d10 which reached 60% and ~32% of the NI baseline value, respectively (Figs. 2a and 2b). Due to the higher baseline values in NI females, radiation-induced thymic suppression was proportionally greater in females than males. Similar to CBC shown in Figs. 1a–e, there were no sex differences in thymic mass or cellularity during H-ARS. By d30, thymus weight in IR males and females combined was 40% of that in NI mice ($p<0.01$, Fig. 2a). Thymus weights in both NI and IR mice continued to decrease as mice aged, with values from IR mice remaining significantly less than those in NI mice throughout the DEARE phase ($p<0.01$). Parallel trends were observed for thymic cellularity (Fig. 2b).

Naïve T cells migrate from the thymus to the spleen where they encounter foreign antigens and undergo activation. Spleen weight and cellularity reached their nadirs by d3 post-IR, followed by a partial recovery by d20 (Figs. 3a and 3b). Similar to peripheral blood, the reconstitution of spleen in the H-ARS phase was monophasic. Spleen weight and cellularity from both IR survivors and NI mice did not change drastically as mice aged, unlike the age-related involution observed in thymus (Figs. 3a and 3b). The significant increase in female spleen weight with age (Fig. 3a) may be related to the reported enhanced extramedullary hematopoiesis (EMH) in females compared to males (Suttie 2006).

Histological analyses of thymus and spleen

Thymi and spleens from NI and IR mice at different ages were stained by H&E to evaluate histological changes throughout the H-ARS and DEARE phases. The difficulty in detecting thymi of aged radiation survivor mice due to accelerated involution with age, coupled with the increased mortality of aged IR mice, resulted in very limited data for analyses after 12 mo post-IR, so thymus and spleen analyses ended at 12 mo post-IR. Young [3 month old (m/o)] NI thymi were characterized by a large cortex:medulla ratio of 3:1–4:1 with a distinct corticomedullary (CM) junction (Fig. 4a). The cortex thinned significantly after irradiation, such that by d20 post-IR (second nadir) the cortex:medulla ratio dropped to 1:1–2:1 and the CM junction became blurry. Thymi from aged NI mice (15 m/o) also displayed a thin cortex but with a clear CM junction, as well as focal fibrous proliferation. Aged thymi from all H-

ARS survivors [12 months (mo.) post-IR] demonstrated a large mass of adipose tissue and reticular connective tissue surrounding a small, hypocellular thymus with undistinguishable CM junction. The CM junction of aged thymi ranged between 1.1–2.1. Photographs of thymi from NI and IR mice at different ages in Fig. 4a illustrate the vast differences in size.

To further confirm that radiation induces fibrous proliferation in the thymus early post-IR, thymi at 30 days post-IR were stained with Picrosirius red to identify collagen deposition, which was found to be localized to the medulla (Fig. 4b). Quantification with ImageJ revealed 20–30% more collagen deposition in the medulla of IR mice in comparison with NI mice as early as d30 post-IR (Fig. 4b).

The normal adult mouse spleen is comprised of clearly visible white and red pulp compartments with slight to mild EMH present in the red pulp. By d20 post-IR, the white pulp portion had increased in size, disrupting the normal red and white pulp architecture [Fig. 4c and as reported (Brues and Stroud 1964)]. The enlarged white pulp was characterized by diffuse lymphoid cell over-growth and focally mitotic blast cell figures consistent with EMH. Prominent EMH was also observed in 15-month-old NI and DEARE spleens, likely contributing to the maintenance of spleen size as mice aged, unlike the aging thymus which undergoes involution. The low power magnification and resolution used for the images in Fig. 4c does not allow visualization of EMH.

Phenotypic analyses of lymphoid compartments

The authors have previously documented significantly decreased PB lymphocytes in H-ARS survivors, which correlated with significant myeloid skew (Chua et al. 2019) and decreased number of functional BM-derived lymphoid progenitors (Chua et al. 2012). To better understand the effects of lethal radiation exposure on specific lymphoid subpopulations, primitive lymphocyte populations were phenotypically defined and enumerated in PB, thymus, spleen, and BM of aged H-ARS survivors in comparison to age-matched NI controls and young NI mice. Representative flow cytometric gating strategies are shown for all these phenotypes in Fig. S1. Aged H-ARS survivors exhibited significantly decreased numbers of PB B220+ B cells, CD4+ T cells, CD4+ naïve cells, and CD8+ naïve T cells compared to age-matched NI controls (Figs. 5a, b, d, & e). PB CD8+ cells were also reduced (non-significantly) in H-ARS survivors compared to aged NI controls (Fig. 5c), as were CD4+ memory and CD8+ memory cells (non-significantly; data not shown). Normal aging in NI mice resulted in non-significant reductions in all PB T lymphocyte populations examined in comparison to 3 m/o NI mice (Figs. 5b–e), with an apparent increase in B cells (Fig. 5a). There were no sex differences in numbers of PB lymphocyte subpopulations in any group, so male and female data were combined.

In the spleen, a similar pattern of decreased numbers of CD4+, CD4+ naïve, and CD8+ naïve cells was observed in H-ARS survivors versus NI age-matched controls as in PB, but differences did not reach significance (Figs. 5f, h, & i). More prominent was a significant age-related decrease in CD8+, CD4+ naïve, and CD8+ naïve splenocytes in aged NI mice compared to young NI mice (Figs. 5g–i). There was no difference in the number of CD8+ lymphocytes between aged NI and IR mice, similar to PB (Fig. 5g), and there were no sex differences in splenocyte T cell subgroups.

The age-related and radiation-related decrease in total thymocytes presented in Fig. 2b was also found to exist when thymic subpopulations from males and females were combined: DN, DP, CD4+, CD8+, DN1, DN2, DN3, and DN4 were all significantly decreased in H-ARS survivors compared to NI age-matched controls (Figs. 5j–q). Likewise, all these populations were significantly decreased in aged NI mice compared to young NI mice (again, combining data from males and females), illustrating the normal age-related thymic involution (Figs. 5j–q). Of interest, sex differences in thymic subpopulations were found to exist. In agreement with others (Aspinall and Andrew 2001), 3 m/o females had more DP cells than males (Fig. 5k). In addition, all thymic subpopulations trended higher in male H-ARS survivors compared to females, similar to the increased PB CBC in males versus females, and these differences reached significance for DN, DP, CD4+, and DN3 cells (Figs. 5j–I & p).

Peripheral lymphocytes originate from primitive BM progenitors termed LMPP and CLP, which originate from multi-potent LT-HSC. To better understand BM involvement in immune deficiencies, BM LMPP and CLP were enumerated in H-ARS survivors in comparison to age-matched NI mice and young NI controls. Both frequency [as a percentage of Lin^{-} c-Kit^{hi} Sca-1^{hi} (LSK) cells] and absolute number of LMPP and CLP were significantly decreased in H-ARS survivors compared to age-matched controls (Figs. 5r–u). In NI mice, LMPP and CLP frequencies were also found to decrease significantly with age (Fig. 5r & 5s), as previously reported (Grover et al. 2016, Xiao et al. 2016). However, when calculated as a percentage of whole BM, the percentages of both LMPP and CLP were found to be two-fold higher in aged NI mice compared to young NI (LMPP of old vs young: 0.04 ± 0.009% vs 0.02 ± 0.005%, p=0.02; CLP of old vs. young: 0.013 ± 0.0029 vs. 0.007 ± 0.0015%, p=0.06). Similarly, absolute numbers of LMPP and CLP were 5-fold and 6-fold increased in old vs. young NI mice, respectively (Figs. 5t & 5u). This apparent dichotomy between decreased frequency and increased number can be explained by the significant phenotypic expansion of LT-HSC with age, as we (Chua et al. 2019) and others (Rossi et al. 2005) have reported, despite declining functional potential (Morrison et al. 1996, Kim et al. 2003, Kamminga et al. 2005, Nijnik et al. 2007, Rossi et al. 2007, Rube et al. 2011, Chua et al. 2012, Snoeck 2013, Behrens et al. 2014, Chua et al. 2019). No sex differences were observed in the frequency or number of BM lymphoid progenitors.

DISCUSSION

Lymphoid organs and lymphocytes are highly radiosensitive (Trowell 1952) due in part to their propensity toward rapid apoptosis when exposed to radiation. The acute effects of radiation exposure on the lymphoid system are well known, but the late effects and long-term immune suppression in survivors of H-ARS are less well characterized (Kusunoki and Hayashi 2008, Farese et al. 2015, Chua et al. 2019). In this report, radiation damage was investigated at all levels of lymphopoiesis in both male and female long term H-ARS survivors, and was found to be characterized by significant tissue-specific reconstitution and involution patterns, age-related differences, and noteworthy male/female differences, especially in the thymus.

The authors previously reported persistent long-term dysfunction in competitive transplantation assays of phenotypically defined BM LT-HSC isolated from H-ARS survivors. Of note, lymphoid reconstitution in recipients of these BM LT-HSC transplants was severely diminished (Chua et al. 2012, Chua et al. 2019), illustrating the loss of multi-lineage reconstitution potential of LT-HSC from DEARE mice. Herein, the primitive BM progenitors LMPP and CLP, direct progeny of LT-HSC, were enumerated and found to be significantly decreased in frequency and absolute number in DEARE mice, strongly implicating LT-HSC dysfunction as a significant contributor to the diminished lymphoid reconstitution in DEARE mice.

Peripheral blood reconstitution in long term H-ARS survivors was marked by significant myeloid skew, as previously reported (Farese et al. 2015, Chua et al. 2019), and found herein to be present in both males and females. Of interest, myeloid skew was found to be more severe in IR females compared to males, and was characterized by a steady decline in lymphocyte number beginning around 9 months of age. Declining PB LY numbers in IR females paralleled observations in the thymus, which also showed worse recovery of most classes of thymocytes (DN, DP, CD4+, CD8+ cells) in females, illustrating curious sex differences in immune reconstitution in the DEARE phase. Phenotypic analyses of PB LY subpopulations of DEARE mice revealed that the loss of LY was primarily due to significant loss of B cells, CD4+ T cells, and both CD4+ and CD8+ naïve T cells compared to NI age-matched controls. The LY subpopulation least affected by radiation exposure was CD8+ T cells, which are known to undergo homeostatic peripheral expansion in lymphopenic environments (Li et al. 2007, Min 2018). Similar trends in these LY subpopulations were also present in spleen.

A biphasic recovery pattern of thymocytes was documented during the H-ARS phase with recovery to only ~40% of baseline values, similar to other reports (Takada et al. 1969, Huiskamp et al. 1983). The first spike of cellularity in the biphasic recovery pattern is thought to be due to proliferation of remaining thymocytes (Kadish and Basch 1976, Hiesche and Revesz 1979), which eventually deplete (Harris and Ford 1964, Dukor et al. 1965). This depletion, along with lack of BM support (Blomgren and Revesz 1968), leads to the second nadir. Thymic precursors migrating from the bone marrow to the thymus are responsible for eventual reconstitution (Hiesche and Revesz 1979, Coggle 1981). However, in our H-ARS model with its high dose radiation, BM insufficiency is evident (Chua et al. 2012, Chua et al. 2019), leading to long term thymic insufficiency. The observed increase in medullary fibrosis in the thymus also likely contributes to thymic dysfunction in long term H-ARS survivors. Thymic fibrosis early post-irradiation has also been reported in non-human primate radiation models (Zhang et al. 2015).

Interesting male/female differences were also documented in normal NI C57BL/6 mice. First, males possessed significantly increased numbers of most PB CBC parameters compared to females (WBC, NE, LY, and PLT), and these sex differences persisted into old age. For LY, these differences intensified as mice aged, leading to more severe myeloid skew in NI geriatric females than in males. The presence of myeloid skew in both NI aged mice and H-ARS survivors illustrates similarities between normal aging and radiation damage on hematopoiesis (Hernández et al. 2015, Chua et al. 2019). The decrease in LY in aged NI

mice was primarily due to a decline in all classes of T cells, while B cells increased, as previously shown (Pinchuk and Filipov 2008, Youm et al. 2016). Evidence of homeostatic peripheral expansion of PB CD8+ T cells was also present in aged NI mice. While most thymus parameters (mass, cellularity and T cell subpopulations) were increased in young NI females compared to males [in agreement with others (Kajioka et al. 2000, Aspinall and Andrew 2001) and consistent with human data (Pido-Lopez et al. 2001)], these differences diminished as mice aged. Spleen also showed decreased numbers of T cell subpopulations with age in both sexes, but significantly increased spleen mass in NI aged females. The increase in spleen mass in aged females may be related to the reported increase in EMH in females compared to males (Ramaiah et al. 2018), and is likely due to sex hormone differences between females and males (Oguro et al. 2017). Sex differences in PB and thymus parameters were both abolished after radiation exposure.

Sex differences in lymphoid organs (Kajioka et al. 2000) and age-related thymic involution (Dooley and Liston 2012) have been postulated to be due to sex hormones, which may be further exacerbated by radiation damage to sex organs. Other factors independent of sex hormones, such as sex chromosomes, may also contribute to the observed sex differences. Many genes implicated in immune function are located on the X chromosome, including the interleukin-2 receptor gamma chain gene (Noguchi et al. 1993) which participates in signal transduction of a number of cytokines, and *FOXP3* gene which is involved in regulatory T cell development (Gui et al. 2012). The X chromosome in general imparts an immunological advantage to females in the face of various immune challenges, but can also lead to increased autoimmune diseases (Libert et al. 2010). In addition, radiation-induced epigenetic changes in the murine thymus have been shown to differ between males and females (Pogribny et al. 2005), which may also contribute to sex-related differences in the radiation response and immune reconstitution. Taken together, this study has defined the prolonged immunosuppression at all levels of lymphocyte development in established murine H-ARS and DEARE models. These data build upon previous work by others and add to the understanding of the severe immune dysfunction that occurs in radiation survivors, with the hope that they will be useful for development of potential MCM and therapeutic strategies for radiation-induced long-term immune deficiency.

CONCLUSION

Immune suppression is a serious health risk in individuals exposed to myelosuppressive or ablative radiation, and has not been well-defined in long term survivors of H-ARS. Herein the authors delineated radiation-induced changes in primitive and mature lymphoid cells at all levels of lymphopoiesis in mice exposed to potentially lethal doses of radiation. Tissue-specific reconstitution and involution patterns were documented in PB, thymus, spleen, and BM tissues, along with unique sex-related and age-related changes present in some tissues but not others. The “double hits” of irradiation and age-related stress on lymphopoiesis lead to significant myeloid skew and long-term immune involution. These H-ARS and DEARE mouse models provide useful tools for developing and evaluating medical countermeasures against the immune-suppressing effects of irradiation.

Supplementary Material

Refer to Web version on PubMed Central for supplementary material.

ACKNOWLEDGMENTS

We appreciate the expert histological assistance of Jennifer Stashevsky and the helpful advice of Dr. Joseph Unthank on analyses of thymic tissues using picrosirius red staining.

This project has been funded in whole or in part with federal funds from the National Institute of Allergy and Infectious Diseases (NIAID) under contracts HHSN266200500043C and HHSN272201000046C and grants 1U01AI107340-01 and 2R44 AI088288-03A1, and National Institute on Aging (NIA) under grant R01AG046246-01, National Institutes of Health, Department of Health and Human Services, and the Department of Defense under grants PR140896, PR141527, and PR140433P1.

REFERENCES

Aspinall R and Andrew D. Gender-related differences in the rates of age associated thymic atrophy. Dev Immunol 8: 95–106; 2001. [PubMed: 11589313]

Behrens A, van Deursen JM, Rudolph KL and Schumacher B. Impact of genomic damage and ageing on stem cell function. Nat Cell Biol 16: 201–207; 2014 DOI:10.1038/ncb2928 [PubMed: 24576896]

Bhatia S, Robison LL, Oberlin O, Greenberg M, Bunin G, Fossati-Bellani F and Meadows AT. Breast cancer and other second neoplasms after childhood Hodgkin's disease. N Engl J Med 334: 745–751; 1996 DOI:10.1056/nejm199603213341201 [PubMed: 8592547]

Blomgren H and Revesz L. Cellular composition of mouse thymus after x-ray exposure. Exp Cell Res 51: 92–104; 1968 DOI:10.1016/0014-4827(68)90161-4 [PubMed: 5661954]

Brues AM and Stroud AN. QUANTITATION OF CELLULAR RESPONSES IN THE MOUSE SPLEEN AFTER IRRADIATION*. Annals of the New York Academy of Sciences 114: 557–570; 1964 DOI:10.1111/j.1749-6632.1964.tb53608.x [PubMed: 14125997]

Chua HL, Plett PA, Fisher A, Sampson CH, Vemula S, Feng H, Sellamuthu R, Wu T, MacVittie TJ and Orschell CM. Lifelong residual bone marrow damage in murine survivors of the hematopoietic acute radiation syndrome (H-ARS): a compilation of studies comprising the Indiana University experience. Health Physics 116: 546–557; 2019. [PubMed: 30789496]

Chua HL, Plett PA, Sampson CH, Joshi M, Tabbey R, Katz BP, MacVittie TJ and Orschell CM. Long-Term Hematopoietic Stem Cell Damage in a Murine Model of the Hematopoietic Syndrome of the Acute Radiation Syndrome. Health Physics 103: 356–366 310.1097/HP.1090b1013e3182666d3182666f; 2012. [PubMed: 22929468]

Chua HL, Plett PA, Sampson CH, Katz BP, Carnathan GW, MacVittie TJ, Lenden K and Orschell CM. Survival efficacy of the pegylated G-CSF Maxy-G34 and Neulasta in a mouse model of lethal H-ARS, and residual bone marrow damage in treated survivors. Health Phys 106: 21–38; 2014 DOI:10.1097/HP.0b013e3182a4df10 [PubMed: 24276547]

Coggle JE. The absence of late effects of radiation on the cellularity of the mouse thymus. Int J Radiat Biol Relat Stud Phys Chem Med 40: 229–232; 1981. [PubMed: 6974151]

Dainiak N, Waselenko JK, Armitage JO, MacVittie TJ and Farese AM. The hematologist and radiation casualties. Hematology: 473–496; 2003. [PubMed: 14633795]

Denkinger MD, Leins H, Schirmbeck R, Florian MC and Geiger H. HSC Aging and Senescent Immune Remodeling. Trends Immunol 36: 815–824; 2015 DOI:10.1016/j.it.2015.10.008 [PubMed: 26611154]

Dooley J and Liston A. Molecular control over thymic involution: from cytokines and microRNA to aging and adipose tissue. Eur J Immunol 42: 1073–1079; 2012 DOI:10.1002/eji.201142305 [PubMed: 22539280]

Dukor P, Miller JF, House W and Allman V. Regeneration of thymus grafts. I. Histological and cytological aspects. Transplantation 3: 639–668; 1965 DOI:10.1097/00007890-196509000-00006 [PubMed: 5828539]

Dynlacht JR, Garrett J, Joel R, Lane K, Mendonca MS and Orschell CM. Further Characterization of the Mitigation of Radiation Lethality by Protective Wounding. Radiat Res 187: 732–742; 2017 DOI:10.1667/RR14725.1 [PubMed: 28437188]

Farese AM, Cohen MV, Katz BP, Smith CP, Gibbs A, Cohen DM and MacVittie TJ. Filgrastim improves survival in lethally irradiated nonhuman primates. Radiat Res 179: 89–100; 2013 DOI:10.1667/rr3049.1 [PubMed: 23210705]

Farese AM, Hankey KG, Cohen MV and MacVittie TJ. Lymphoid and Myeloid Recovery in Rhesus Macaques Following Total Body X-Irradiation. Health Physics 109: 414–426; 2015 DOI:10.1097/hp.0000000000000348 [PubMed: 26425902]

Fish BL, Gao F, Narayanan J, Bergom C, Jacobs ER, Cohen EP, Moulder JE, Orschell CM and Medhora M. Combined Hydration and Antibiotics with Lisinopril to Mitigate Acute and Delayed High-dose Radiation Injuries to Multiple Organs. Health Physics 111: 410–419; 2016 DOI:10.1097/hp.0000000000000554 [PubMed: 27682899]

Garrett J, Orschell CM, Mendonca MS, Bigsby RM and Dynlacht JR. Subcutaneous wounding postirradiation reduces radiation lethality in mice. Radiat Res 181: 578–583; 2014 DOI:10.1667/rr13267.1 [PubMed: 24811864]

Garrett J, Sampson CH, Plett PA, Crisler R, Parker J, Venezia R, Chua HL, Hickman DL, Booth C, MacVittie T, Orschell CM and Dynlacht JR. Characterization and Etiology of Swollen Muzzles in Irradiated Mice. Radiat Res 191: 31–42; 2019 DOI:10.1667/rr14724.1 [PubMed: 30339056]

Germain RN. T-cell development and the CD4-CD8 lineage decision. Nat Rev Immunol 2: 309–322; 2002 DOI:10.1038/nri798 [PubMed: 12033737]

Grover A, Sanjuan-Pla A, Thongjuea S, Carrelha J, Giustacchini A, Gambardella A, Macaulay I, Mancini E, Luis TC, Mead A, Jacobsen SE and Nerlov C. Single-cell RNA sequencing reveals molecular and functional platelet bias of aged haematopoietic stem cells. Nat Commun 7: 11075; 2016 DOI:10.1038/ncomms11075 [PubMed: 27009448]

Gui J, Morales AJ, Maxey SE, Bessette KA, Ratcliffe NR, Kelly JA and Craig RW. MCL1 increases primitive thymocyte viability in female mice and promotes thymic expansion into adulthood. Int Immunol 23: 647–659; 2011 DOI:10.1093/intimm/dxr073 [PubMed: 21937457]

Gui J, Mustachio LM, Su DM and Craig RW. Thymus Size and Age-related Thymic Involution: Early Programming, Sexual Dimorphism, Progenitors and Stroma. Aging Dis 3: 280–290; 2012. [PubMed: 22724086]

Guo D, Ye Y, Qi J, Tan X, Zhang Y, Ma Y and Li Y. Age and sex differences in microRNAs expression during the process of thymus aging. Acta Biochimica et Biophysica Sinica 49: 409–419; 2017 DOI:10.1093/abbs/gmx029 [PubMed: 28369179]

Hankey KG, Farese AM, Blaauw EC, Gibbs AM, Smith CP, Katz BP, Tong Y, Prado KL and MacVittie TJ. Pegfilgrastim Improves Survival of Lethally Irradiated Nonhuman Primates. Radiat Res 183: 643–655; 2015 DOI:10.1667/rr13940.1 [PubMed: 26035709]

Harris JE and Ford CE. CELLULAR TRAFFIC OF THE THYMUS: EXPERIMENTS WITH CHROMOSOME MARKERS. EVIDENCE THAT THE THYMUS PLAYS AN INSTRUCTIONAL PART. Nature 201: 884–885; 1964 DOI:10.1038/201884a0 [PubMed: 14132779]

Hernández L, Terradas M, Camps J, Martín M, Tusell L and Genescà A. Aging and radiation: bad companions. Aging Cell 14: 153–161; 2015 DOI:10.1111/acel.12306 [PubMed: 25645467]

Hiesche KD and Revesz L. Effect of cortisone and X-irradiation on cellular depletion and regeneration in the thymus of mice: experimental discrimination between thymus lymphocyte precursors in the bone marrow and in the thymus. Pathol Res Pract 164: 157–166; 1979 DOI:10.1016/s0344-0338(79)80020-5 [PubMed: 461225]

Hoggatt J, Singh P, Stilger KN, Plett PA, Sampson CH, Chua HL, Orschell CM and Pelus LM. Recovery from hematopoietic injury by modulating prostaglandin E(2) signaling post-irradiation. Blood Cells Mol Dis 50: 147–153; 2013 DOI:10.1016/j.bcmd.2012.11.006 [PubMed: 23206586]

Huiskamp R, Davids JAG and Vos O. Short- and Long-Term Effects of Whole-Body Irradiation with Fission Neutrons or X Rays on the Thymus in CBA Mice. Radiat Res 95: 370–381; 1983 DOI:10.2307/3576262 [PubMed: 6351158]

Jones JW, Alloush J, Sellamuthu R, Chua HL, MacVittie TJ, Orschell CM and Kane MA. Effect of gender on biomarker response in a mouse model of the hematopoietic acute radiation syndrome. Health Phys 116: 484–502; 2019 DOI:10.1097/hp.0000000000000961 [PubMed: 30681425]

Kadish JL and Basch RS. Hematopoietic thymocyte precursors. I. Assay and kinetics of the appearance of progeny. J Exp Med 143: 1082–1099; 1976 DOI:10.1084/jem.143.5.1082 [PubMed: 4575]

Kajioka EH, Andres ML, Nelson GA and Gridley DS. Immunologic variables in male and female C57BL/6 mice from two sources. Comp Med 50: 288–291; 2000. [PubMed: 10894494]

Kamiya K, Ozasa K, Akiba S, Niwa O, Kodama K, Takamura N, Zaharieva EK, Kimura Y and Wakeford R. Long-term effects of radiation exposure on health. Lancet 386: 469–478; 2015 DOI:10.1016/s0140-6736(15)61167-9 [PubMed: 26251392]

Kamminga LM, Van Os R, Ausema A, Noach EJK, Weersing E, Dontje B, Vellenga E and De Haan G. Impaired hematopoietic stem cell functioning after serial transplantation and during normal aging. Stem Cells 23: 82–92; 2005 DOI:10.1634/stemcells.2004-0066 [PubMed: 15625125]

Kim M, Moon H-B and Spangrude GJ. Major Age-Related Changes Of Mouse Hematopoietic Stem/Progenitor Cells. Ann N Y Acad Sci 996: 195–208; 2003 DOI:10.1111/j.1749-6632.2003.tb03247.x [PubMed: 12799297]

Kusunoki Y and Hayashi T. Long-lasting alterations of the immune system by ionizing radiation exposure: implications for disease development among atomic bomb survivors. Int J Radiat Biol 84: 1–14; 2008 DOI:10.1080/09553000701616106 [PubMed: 17852558]

Li CR, Santoso S and Lo DD. Quantitative analysis of T cell homeostatic proliferation. Cell Immunol 250: 40–54; 2007 DOI:10.1016/j.cellimm.2008.01.003 [PubMed: 18313651]

Libert C, Dejager L and Pinheiro I. The X chromosome in immune functions: when a chromosome makes the difference. Nat Rev Immunol 10: 594–604; 2010 DOI:10.1038/nri2815 [PubMed: 20651746]

Min BH. Spontaneous T Cell Proliferation: A Physiologic Process to Create and Maintain Homeostatic Balance and Diversity of the Immune System. Front. Immunol 19: 547; 2018.

Morrison SJ, Wandycz AM, Akashi K, Globerson A and Weissman IL. The aging of hematopoietic stem cells. Nat Med 2: 1011–1016; 1996. [PubMed: 8782459]

Nijnik A, Woodbine L, Marchetti C, Dawson S, Lambe T, Liu C, Rodrigues NP, Crockford TL, Cabuy E, Vindigni A, Enver T, Bell JI, Slijepcevic P, Goodnow CC, Jeggo PA and Cornall RJ. DNA repair is limiting for haematopoietic stem cells during ageing. Nature 447: 686–690; 2007 DOI:10.1038/Nature05875 [PubMed: 17554302]

Noguchi M, Yi H, Rosenblatt HM, Filipovich AH, Adelstein S, Modi WS, McBride OW and Leonard WJ. Interleukin-2 receptor gamma chain mutation results in X-linked severe combined immunodeficiency in humans. Cell 73: 147–157; 1993 DOI:10.1016/0092-8674(93)90167-o [PubMed: 8462096]

Oguro H, McDonald JG, Zhao Z, Umetani M, Shaul PW and Morrison SJ. 27-Hydroxycholesterol induces hematopoietic stem cell mobilization and extramedullary hematopoiesis during pregnancy. J Clin Invest 127: 3392–3401; 2017 DOI:10.1172/jci94027 [PubMed: 28783041]

Patchen ML. Amifostine plus granulocyte colony-stimulating factor therapy enhances recovery from supralethal radiation exposures: preclinical experience in animals models. European Journal of Cancer (supplement) 31: S17–S21; 1995.

Pido-Lopez J, Imami N and Aspinall R. Both age and gender affect thymic output: more recent thymic migrants in females than males as they age. Clin Exp Immunol 125: 409–413; 2001. [PubMed: 11531948]

Pinchuk LM and Filipov NM. Differential effects of age on circulating and splenic leukocyte populations in C57BL/6 and BALB/c male mice. Immun Ageing 5: 1; 2008 DOI:10.1186/1742-4933-5-1 [PubMed: 18267021]

Plett PA, Chua HL, Sampson CH, Katz BP, Fam CM, Anderson LJ, Cox G and Orschell CM. PEGylated G-CSF (BBT-015), GM-CSF (BBT-007), and IL-11 (BBT-059) analogs enhance survival and hematopoietic cell recovery in a mouse model of the Hematopoietic Syndrome of the Acute Radiation Syndrome. Health Phys 106: 7–20; 2014 DOI:10.1097/HP.0b013e3182a4dd4e [PubMed: 24276546]

Plett PA, Sampson CH, Chua HL, Jackson W, Vemula S, Sellamuthu R, Fisher A, Feng H, Wu T, MacVittie TJ and Orschell CM. The H-ARS Dose Response Relationship (DRR): Validation and Variables. Health Physics 109: 391–398; 2015 DOI:10.1097/hp.0000000000000354 [PubMed: 26425900]

Plett PA, Sampson CH, Chua HL, Joshi M, Booth C, Gough A, Johnson CS, Katz BP, Farese AM, Parker J, MacVittie TJ and Orschell CM. Establishing a Murine Model of the Hematopoietic Syndrome of the Acute Radiation Syndrome. Health Physics 103: 343–355 310.1097/HP.1090b1013e3182667309; 2012. [PubMed: 22929467]

Pogribny I, Koturbash I, Tryndyak V, Hudson D, Stevenson SM, Sedelnikova O, Bonner W and Kovalchuk O. Fractionated low-dose radiation exposure leads to accumulation of DNA damage and profound alterations in DNA and histone methylation in the murine thymus. Mol Cancer Res 3: 553–561; 2005 DOI:10.1158/1541-7786.Mcr-05-0074 [PubMed: 16254189]

Ramaiah L, Bounous D and Elmore S. Fundamentals of Toxicologic Pathology.Academic Press; 2018.

Rezzani R, Nardo L, Favero G, Peroni M and Rodella LF. Thymus and aging: morphological, radiological, and functional overview. Age (Dordr) 36: 313–351; 2014 DOI:10.1007/s11357-013-9564-5 [PubMed: 23877171]

Rossi DJ, Bryder D, Seita J, Nussenzweig A, Hoeijmakers J and Weissman IL. Deficiencies in DNA damage repair limit the function of haematopoietic stem cells with age. Nature 447: 725–729; 2007 DOI:10.1038/Nature05862 [PubMed: 17554309]

Rossi DJ, Bryder D, Zahn JM, Ahlenius H, Sonu R, Wagers AJ and Weissman IL. Cell intrinsic alterations underlie hematopoietic stem cell aging. Proc Natl Acad Sci U S A 102: 9194–9199; 2005 DOI:10.1073/pnas.0503280102 [PubMed: 15967997]

Rube CE, Fricke A, Widmann TA, Furst T, Madry H, Pfreundschuh M and Rube C. Accumulation of DNA damage in hematopoietic stem and progenitor cells during human aging. PLoS One 6: e17487; 2011 DOI:10.1371/journal.pone.0017487 [PubMed: 21408175]

Sasaki H, Kodama K and Yamada M. A review of forty-five years study of Hiroshima and Nagasaki atomic bomb survivors. Aging. J Radiat Res 32 Suppl: 310–326; 1991. [PubMed: 1762120]

Satyamitra M, Kumar VP, Biswas S, Cary L, Dickson L, Venkataraman S and Ghosh SP. Impact of Abbreviated Filgrastim Schedule on Survival and Hematopoietic Recovery after Irradiation in Four Mouse Strains with Different Radiosensitivity. Radiat Res 187: 659–671; 2017 DOI:10.1667/rr14555.1 [PubMed: 28362168]

Sempowski GD, Gooding ME, Liao HX, Le PT and Haynes BF. T cell receptor excision circle assessment of thymopoiesis in aging mice. Mol Immunol 38: 841–848; 2002. [PubMed: 11922942]

Shakhov AN, Singh VK, Bone F, Cheney A, Kononov Y, Krasnov P, Bratanova-Toshkova TK, Shakhova VV, Young J, Weil MM, Panoskaltsis-Mortari A, Orschell CM, Baker PS, Gudkov A and Feinstein E. Prevention and mitigation of acute radiation syndrome in mice by synthetic lipopeptide agonists of Toll-like receptor 2 (TLR2). PLoS One 7: e33044; 2012 DOI:10.1371/journal.pone.0033044 [PubMed: 22479357]

Singh VK and Seed TM. Pharmacological management of ionizing radiation injuries: current and prospective agents and targeted organ systems. Expert Opin Pharmacother 21: 317–337; 2020 DOI:10.1080/14656566.2019.1702968 [PubMed: 31928256]

Snoeck HW. Aging of the hematopoietic system. Curr Opin Hematol 20: 355–361; 2013 DOI:10.1097/MOH.0b013e3283623c77 [PubMed: 23739721]

Suttie AW. Histopathology of the spleen. Toxicol Pathol 34: 466–503; 2006 DOI:10.1080/01926230600867750 [PubMed: 17067940]

Takada A, Takada Y, Huang CC and Ambrus JL. Biphasic pattern of thymus regeneration after whole-body irradiation. J Exp Med 129: 445–457; 1969. [PubMed: 4886041]

Trowell OA. The sensitivity of lymphocytes to ionising radiation. The Journal of Pathology and Bacteriology 64: 687–704; 1952 DOI:10.1002/path.1700640403 [PubMed: 13000583]

Unthank JL, Miller SJ, Quickery AK, Ferguson EL, Wang M, Sampson CH, Chua HL, DiStasi MR, Feng H, Fisher A, Katz BP, Plett PA, Sandusky GE, Sellamuthu R, Vemula S, Cohen EP, MacVittie TJ and Orschell CM. Delayed Effects of Acute Radiation Exposure in a Murine Model

of the H-ARS: Multiple-Organ Injury Consequent to <10 Gy Total Body Irradiation. Health Physics 109: 511–521; 2015 DOI:10.1097/hp.0000000000000357 [PubMed: 26425910]

Unthank JL, Ortiz M, Trivedi H, Pelus LM, Sampson CH, Sellamuthu R, Fisher A, Chua HL, Plett A, Orschell CM, Cohen EP and Miller SJ. Cardiac and Renal Delayed Effects of Acute Radiation Exposure: Organ Differences in Vasculopathy, Inflammation, Senescence and Oxidative Balance. Radiat Res 191: 383–397; 2019 DOI:10.1667/rr15130.1 [PubMed: 30901530]

van Heijst JW, Ceberio I, Lipuma LB, Samilo DW, Wasilewski GD, Gonzales AM, Nieves JL, van den Brink MR, Perales MA and Pamer EG. Quantitative assessment of T cell repertoire recovery after hematopoietic stem cell transplantation. Nat Med 19: 372–377; 2013 DOI:10.1038/nm.3100 [PubMed: 23435170]

Vogel B, Siebert H, Hofmann U and Frantz S. Determination of collagen content within picrosirius red stained paraffin-embedded tissue sections using fluorescence microscopy. MethodsX 2: 124–134; 2015 DOI:10.1016/j.mex.2015.02.007 [PubMed: 26150980]

Xiao J, Zhou H, Wu N and Wu L. The non-canonical Wnt pathway negatively regulates dendritic cell differentiation by inhibiting the expansion of Flt3(+) lymphocyte-primed multipotent precursors. Cell Mol Immunol 13: 593–604; 2016 DOI:10.1038/cmi.2015.39 [PubMed: 26051474]

Youm YH, Horvath TL, Mangelsdorf DJ, Kliewer SA and Dixit VD. Prolongevity hormone FGF21 protects against immune senescence by delaying age-related thymic involution. Proc Natl Acad Sci U S A 113: 1026–1031; 2016 DOI:10.1073/pnas.1514511113 [PubMed: 26755598]

Zhang P, Cui W, Hankey KG, Gibbs AM, Smith CP, Taylor-Howell C, Kearney SR and MacVittie TJ. Increased Expression of Connective Tissue Growth Factor (CTGF) in Multiple Organs After Exposure of Non-Human Primates (NHP) to Lethal Doses of Radiation. Health Phys 109: 374–390; 2015 DOI:10.1097/hp.0000000000000343 [PubMed: 26425899]

Zlotoff DA and Bhandoola A. Hematopoietic progenitor migration to the adult thymus. Ann N Y Acad Sci 1217: 122–138; 2011 DOI:10.1111/j.1749-6632.2010.05881.x [PubMed: 21251013]

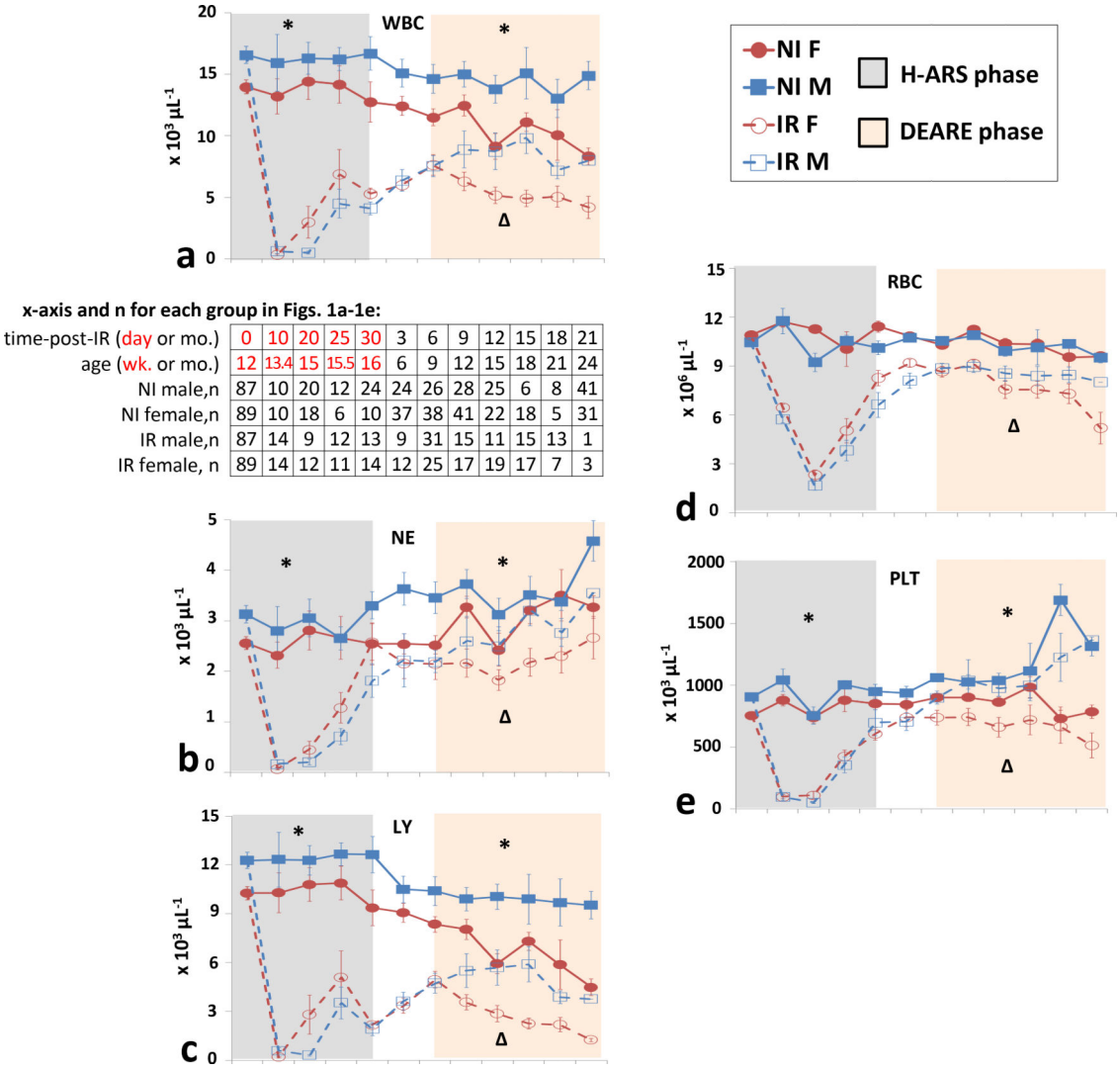

x-axis and n for each group in Figs. 1a-1e:

time-post-IR (day or mo.)	0	10	20	25	30	3	6	9	12	15	18	21
age (wk. or mo.)	12	13.4	15	15.5	16	6	9	12	15	18	21	24
NI male,n	87	10	20	12	24	24	26	28	25	6	8	41
NI female,n	89	10	18	6	10	37	38	41	22	18	5	31
IR male,n	87	14	9	12	13	9	31	15	11	15	13	1
IR female, n	89	14	12	11	14	12	25	17	19	17	7	3

Fig. 1. Reconstitution of the peripheral blood post-IR.

Peripheral blood was harvested from C57Bl/6 mice that had received a single TBI dose of 8.72 or 9.04 Gy gamma radiation at 12 weeks of age (IR) and from age-matched NI controls at various time-points. NI and IR mice were evaluated for WBC (panel a), NE (panel b), LY (panel c), RBC (panel d), PLT (panel e) and analyzed separately by sex. Data are mean ± SEM. Asterisk (*) indicates $p<0.05$ comparing female (F) with male (M) in NI group. Triangle (Δ) indicates $p<0.05$ comparing F with M in IR group. All data are significantly different between NI and IR mice and thus not indicated on each graph. Time post-IR, age, and number of mice analyzed at each time point are shown in the table below panel a. Note that the "n" for time 0 in the table is the same for both NI and IR groups since both NI and IR mice share the same "time 0" data.

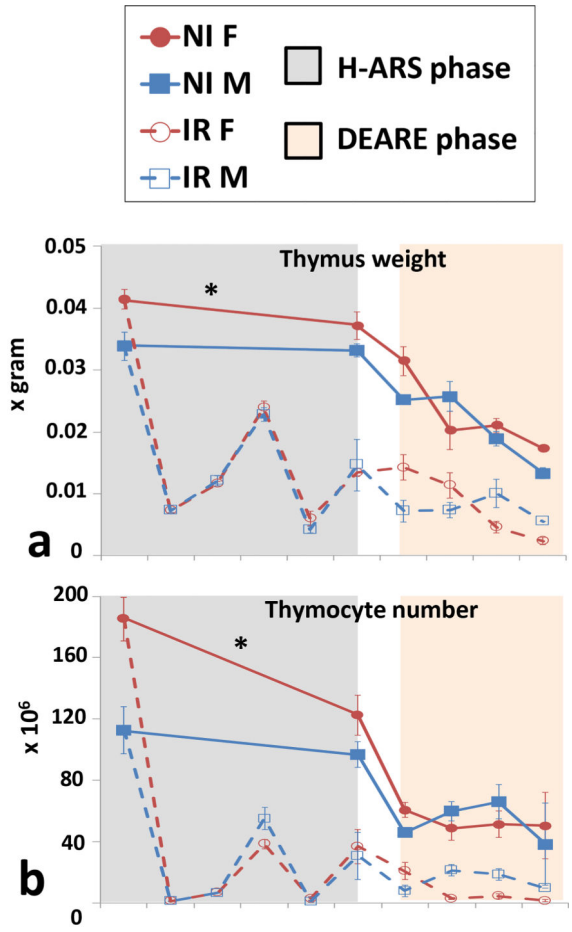

x-axis and n for each group in Figs. 2a-2b:

time-post-IR (day or mo.)	0	3	7	10	20	30	6	9	12	15
age (wk. or mo.)	12	12.4	13	13.4	15	16	9	12	15	18
NI male,n	14	Not done				7	5	7	11	2
NI female,n	18	Not done				6	8	5	12	3
IR male,n	14	16	4	9	6	2	8	3	4	1
IR female, n	18	11	4	10	8	2	11	7	8	3

Fig. 2. Reconstitution and involution in thymus post-IR.

Thymi were harvested from C57Bl/6 mice that had received a single TBI dose of 8.72 or 9.04 Gy gamma radiation at 12 weeks of age (IR) and from age-matched NI controls at various time-points. NI and IR mice were evaluated for thymus weight (panel a) and thymus cellularity (panel b) separately by sex. Data are mean ± SEM. Asterisk (*) indicates $p<0.05$ comparing F with M in NI group. All data are significantly different between NI and IR mice and thus not indicated on each graph. Time post-IR, age, and number of mice analyzed at each time point are given in the table. Note that the “n” for time 0 in the table is the same for both NI and IR groups since both NI and IR mice share the same “time 0” data.

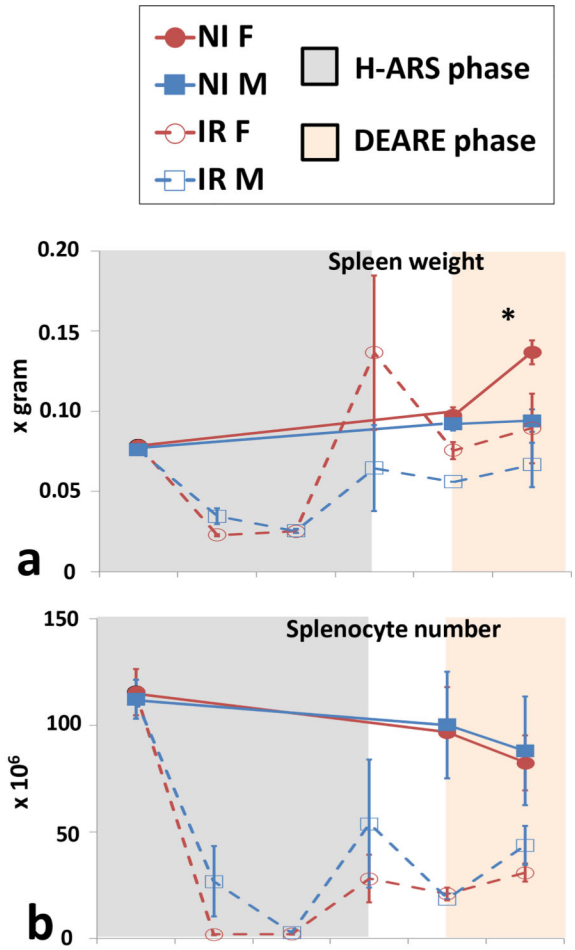

x-axis and n for each group in Figs. 3a-3b:

time-post-IR (day or mo.)	0	3	10	20	6	12
age (wk. or mo.)	12	12.4	13.4	15	9	15
NI male,n	18	Not done			8	9
NI female,n	17	Not done			10	10
IR male,n	18	10	8	3	1	2
IR female, n	17	8	8	5	2	4

Fig. 3. Reconstitution of the spleen post-IR.

Spleens were harvested from C57Bl/6 mice that had received a single TBI dose of 8.72 or 9.04 Gy gamma radiation at 12 weeks of age (IR) and from age-matched NI controls at various time-points. NI and IR mice were evaluated for spleen weight (panel a) and spleen cellularity (panel b) separately by sex. Data are mean ± SEM. Asterisk (*) indicates $p<0.05$ comparing F with M in NI group. All data are significantly different between NI and IR mice and thus not indicated on each graph. Time post-IR, age, and number of mice analyzed at each time point are given in the table. Note that the “n” for time 0 in the table is the same for both NI and IR groups since both NI and IR mice share the same “time 0” data.

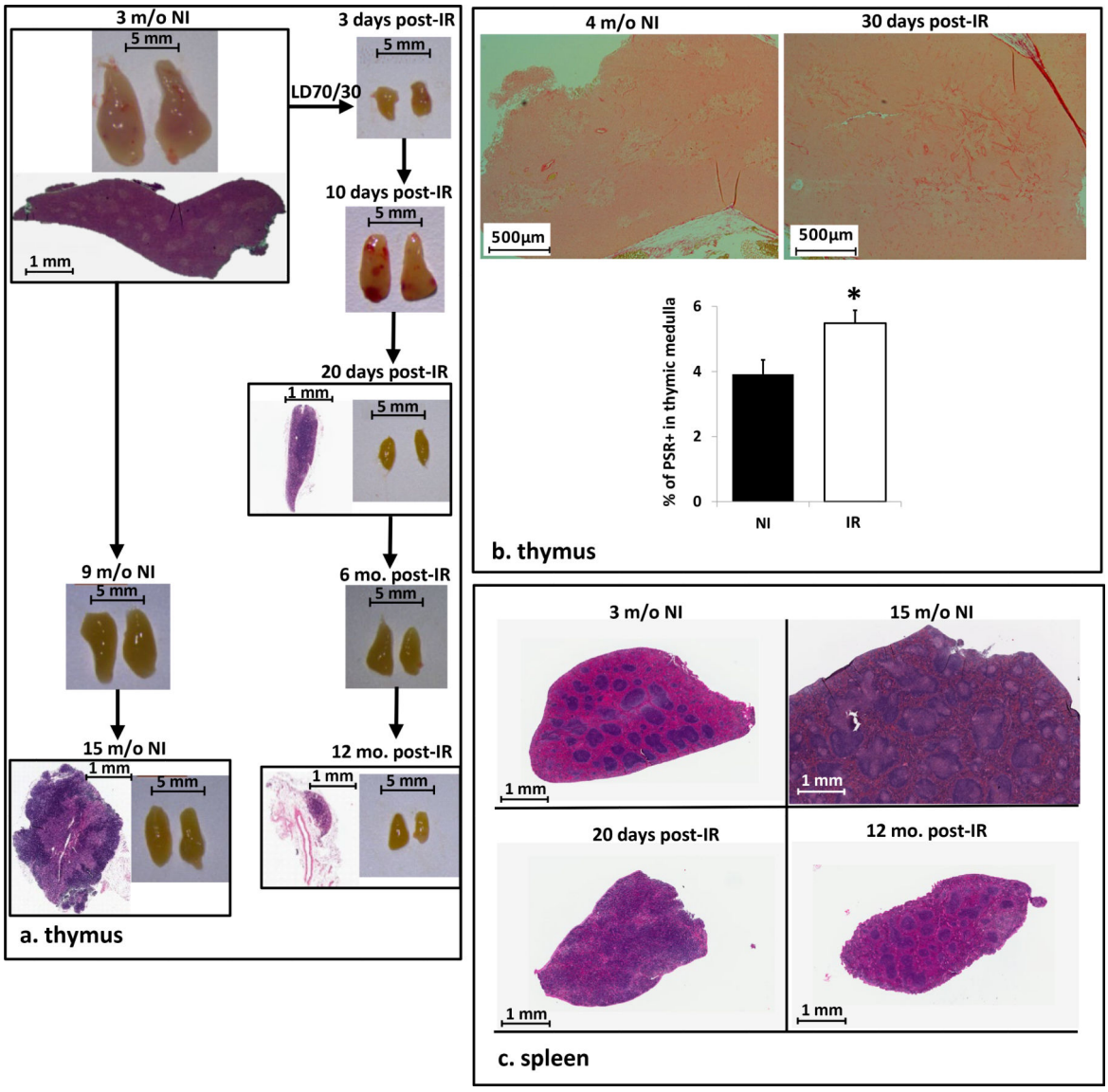

Fig. 4. Images and histology of thymi and spleens in NI and IR mice.

Panel a shows representative photographs of thymi from NI and IR mice at various time-points, and thymi that were fixed in formalin, embedded in paraffin and stained for hematoxylin and eosin. Panel b shows representative micrographs of thymic sections from 4 m/o NI mice and IR mice 30 days post-IR stained with Picrosirius red. Collagen deposition is presented as the percentage of Picrosirius red positive area in the medullary area using ImageJ software. Data are mean ± SEM. *p<0.05 comparing IR and NI mice. n=6 mice per group (2 females and 4 males per group), with one tissue section stained per mouse. Panel c shows spleens from 3 and 15 m/o NI mice and IR mice 20 days and 12 mo. post-IR. Tissues were fixed in formalin, embedded in paraffin and stained for hematoxylin and eosin.

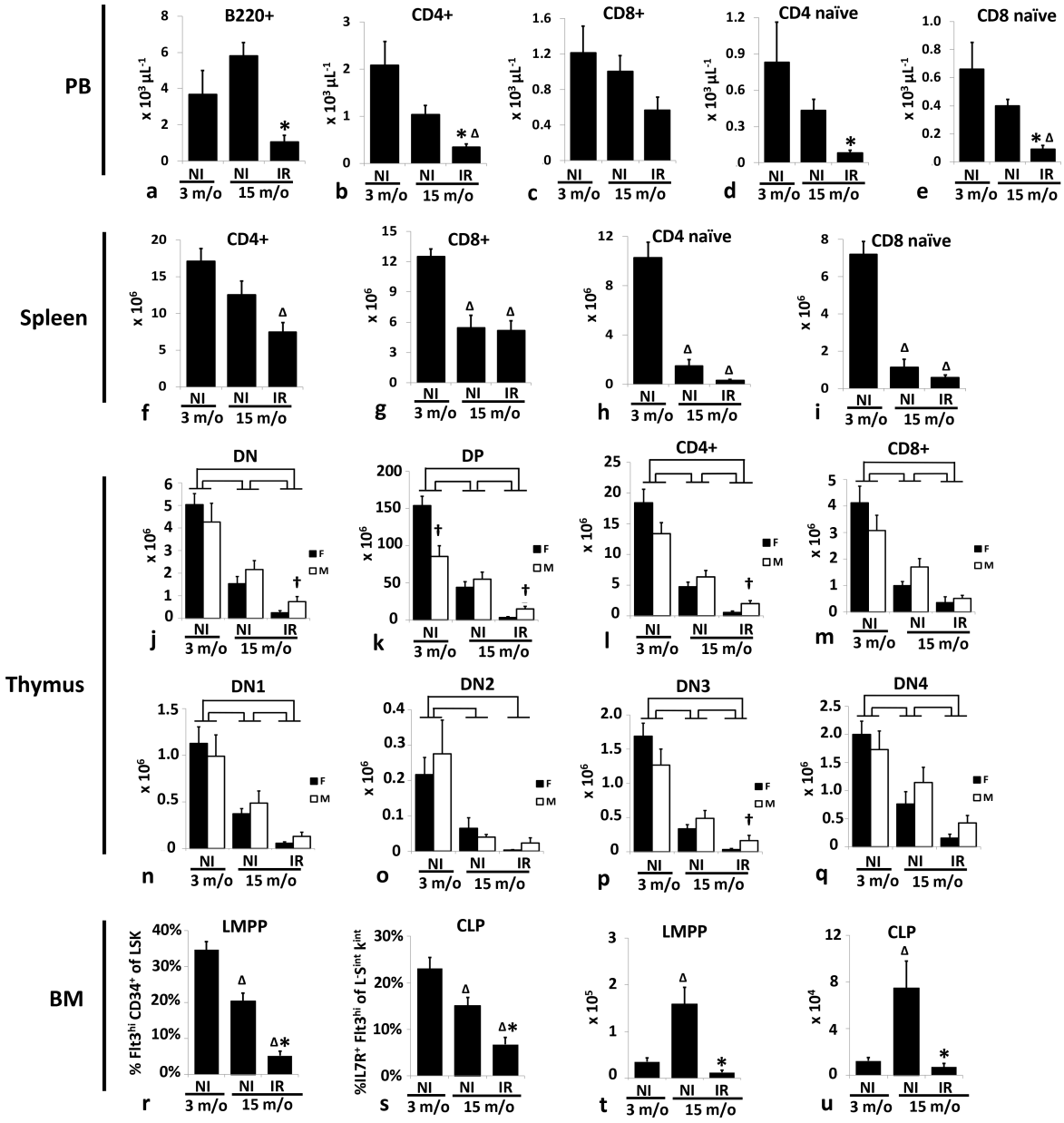

Fig. 5. Lymphocyte subsets in young and aged NI mice and aged H-ARS survivors.

C57Bl/6 mice were exposed to a single TBI dose of 8.72 or 9.04 Gy gamma radiation at 12 w/o and euthanized at 15 m/o, along with 3 m/o and 15 m/o NI mice. Peripheral blood, splenocytes, thymocytes and bone marrow cells were processed and stained with antibodies as described in Materials and Methods. Flow cytometric analyses identifies peripheral blood B220+ cells (panel a), CD4+ T cells (panel b), CD8+ T cells (panel c), CD4 naïve T cells (panel d) and CD8 naïve T cells (panel e); splenic CD4+ T cells (panel f), CD8+ T cells (panel g), CD4 naïve T cells (panel h), and CD8 naïve T cells (panel i); thymic DN (panel j), DP (panel k), CD4+ (panel l), CD8+ (panel m), DN1 (panel n), DN2 (panel o), DN3 (panel p) and DN4 (panel q) cells; and percentages of BM LMPP (panel r) and CLP cells (panel s), and absolute number of LMPP (panel t) and CLP cells (panel u). Data from M and F spleen,

PB, and BM were not significantly different and thus combined. Data are mean ± SEM. Asterisk (*) indicates $p<0.05$ compared to 15 month old NI; triangle (Δ) indicates $p<0.05$ compared to 3 month old NI group in panels a-i and r-u. Brackets (⊓) in panels j-q indicate $p<0.05$ comparing F and M combined data to other groups, and dagger (†) indicates $p<0.05$ comparing F to M within each NI or IR group. n=4–6 mice per group.